Astron. Astrophys. 350, L51–L54 (1999)

ASTRONOMY AND ASTROPHYSICS

LETTER

Letter to the Editor

HST/NICMOS2 observations of the HD 141569 A circumstellar disk⋆

J.C. Augereau[1], **A.M. Lagrange**[1], **D. Mouillet**[1], **and F. Ménard**[1,2]

[1] Laboratoire d'Astrophysique de l'Observatoire de Grenoble, Université J. Fourier / CNRS, B.P. 53, 38041 Grenoble Cedex 9, France
[2] Canada-France-Hawaii Telescope Corporation, PO Box 1597, Kamuela, HI 96743, USA

Received 28 July 1999 / Accepted 22 September 1999

Abstract. We report the first resolved scattered light images of the circumstellar dust disk around the old Pre-Main Sequence star HD 141569 A. The disk seen in HST/NICMOS2 images shapes a bright annulus inclined at $37.5° \pm 4.5°$ from edge-on. This ring peaks at 325 ± 10 AU from the star with a characteristic width of ~ 150 AU. At $1.6\,\mu$m, the dust grains scatter a total flux density of at least 4.5 ± 0.5 mJy. Our disk model using the spatial distribution implied by the images does not explain the $10\,\mu$m excess and requires an additional grain population closer to the star. Some similarities and differences with the dust annulus surrounding HR 4796 A are pointed out.

Key words: stars: individual: HD 141569 A – stars: circumstellar matter

1. Introduction

The recent discovery of a disk around the old Pre-Main Sequence A0 star HR 4796 A (Koerner et al. 1998; Jayawardhana et al. 1998; Augereau et al. 1999a; Schneider et al. 1999) opened new perspectives in our understanding of the evolution of circumstellar disks and the early stages of planetary formation (Lagrange et al. 1999). The comparable age, spectral type and IRAS infrared excess of the post Herbig Ae/Be star HD 141569 A are pertinent clues for suspecting the presence of an optically thin disk around this star at a similar evolutionary status ($t_* \geq 10$ Myr, B9.5Ve star, van den Ancker et al. 1998).

A main difference with HR 4796 A may concern the multiplicity. Whereas HR 4796 A has a physically bounded companion (HR 4796 B), which may play a role in the dynamics of the disk, the two stellar companions of HD 141569 A detected so far (Gahm et al. 1983; Pirzkal et al. 1997) may not be gravitationally linked to the primary, as postulated by Lindroos (1985). In addition, no spectroscopic companion is detected by Corporon & Lagrange (1999).

Since IRAS, further investigations of the material around HD 141569 A have been performed. HD 141569 A shows a very small intrinsic polarization consistent with that of the prototype Vega-like stars (Yudin & Evans 1998; Yudin et al. 1999). Emission spectral features from circumstellar dust grains have also been observed by Sylvester et al. (1996a) at 10–20 μm.

Whereas the spectral energy distribution (SED) constrains the grain composition, it poorly constrains the shape of the dust distribution. In particular, models predict an inner edge for the disk ranging between 10 AU (Malfait et al. 1998) and 650 AU (Sylvester & Skinner 1996b).

In this Letter, we present the first resolved scattered light images of the HD 141569 A circumstellar disk obtained with the coronagraph on the HST/NICMOS2 camera. A disk detection is also reported independently by Weinberger et al. (1999) at $1.1\,\mu$m. We afterwards detail the morphology of the resolved structure, its brightness at $1.6\,\mu$m and finally discuss some disk properties.

2. Observations and reduction procedure

2.1. The data

HST/NICMOS2 coronagraphic observations of HD 141569 A ($V = 7.1$) were obtained on 1998 August 17 in MULTIACCUM mode. Six consecutive exposures on the target were performed in filter F160W (central wavelength $\simeq 1.6\,\mu$m, bandwidth $\simeq 0.4\,\mu$m) corresponding to a total integration time of 14 m 23 s. The reduction procedure of coronagraphic data requires a comparison star to assess the Point Spread Function (PSF). For this, the A1V star HD 145788, which shows no evidence of circumstellar material, was observed during the same orbit for 6 m 24 s to achieve a similar signal to noise ratio given its own flux ($V = 6.25$).

A narrow band (filter F171M) view of the field around HD 141569 A taken during the target acquisition confirms the presence of two bright companions HD 141569 B and HD 141569 C previously identified in K band by Pirzkal et al. (1997) (Fig. 1). Measured position angles (hereafter PA) and separations from the primary star are summarized in Fig. 1. PAs are fully con-

Send offprint requests to: J.C. Augereau

⋆ Based on observations with the NASA/ESA Hubble Space Telescope, obtained at the Space Telescope Science Institute, which is operated by the Association of Universities for Research in Astronomy, Inc. under NASA contract No. NAS5-26555.

Correspondence to: augereau@obs.ujf-grenoble.fr

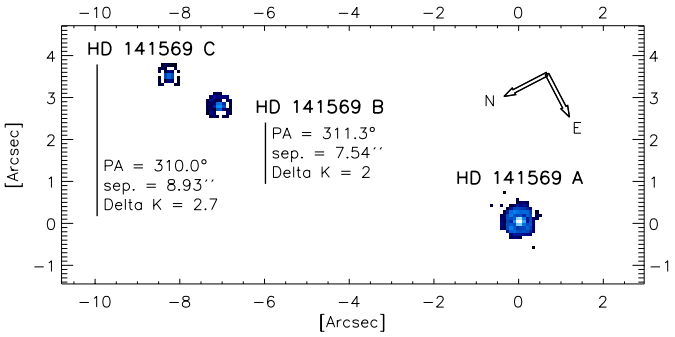

Fig. 1. The multiple system HD 141569 in filter F171M (central wavelength $\simeq 1.72\,\mu$m, bandwidth $\simeq 0.07\,\mu$m) and known astronomical parameters for the companions HD 141569 B and HD 141569 C. K magnitude differences are from Pirzkal et al. (1997).

Table 1. Surface brightness (SB) steepness indexes α (SB $\propto r^{\alpha}$) and corresponding SB ranges in mag.arcsec^{-2} for the Southern extension. The zero point flux in F160W filter given by the STScI is 1113 Jy.

Major Axis Radial Range	Steepness Index α	SB Range in mag.arcsec^{-2}
$2.7'' \rightarrow 3.2''$	$+1.98 \pm 0.14$	$17.3 \rightarrow 16.9$
$3.3'' \rightarrow 3.6''$	-2.32 ± 0.16	$16.9 \rightarrow 17.2$
$3.6'' \rightarrow 4.2''$	-6.87 ± 0.14	$17.2 \rightarrow 18.3$
$4.2'' \rightarrow 6.0''$	-2.75 ± 0.20	$18.3 \rightarrow 19.5$

sistent with Pirzkal et al. (1997) results whereas distances from this work are about 11% larger than those measured by these last authors.

2.2. Reduction procedure for the coronagraphic data: basic cleaning and PSF subtraction

For both HD 141569 A and the PSF reference (HD 145788), we added the calibrated files provided by the STScI. We cleaned the bad pixels and 'grots' (STScI 1997) using ECLIPSE reduction procedures (Devillard 1997). Blurred stripes on the images associated to electronic echos of the source (also called 'Mr Staypuft' ghosts, STScI 1997) were subtracted by averaging a profile perpendicular to the stripes in a region free of astronomical sources.

Before being subtracted, the reference star flux has to be scaled to that of the target object. The ratio of the HD 141569 A image to the reference star image gives the scaling factor. At this stage of the reduction, this is also an *unbiased* and powerful way to detect circumstellar material. Indeed, a circumstellar structure is expected to appear as a continuous feature in the ratio at a level significantly higher than the background level.

Fig. 2 (*left*) shows this ratio. An annular structure centered on the star clearly appears especially in the right and bottom parts of the image whereas the light of the stellar companions (mainly HD 141569 B) contaminates the opposite side. Azimuthally averaged radial profiles on different areas of the ratio confirm the presence of an excess (Fig. 2, *right*).

The true linear resolution is higher in an angular sector close to the major axis of the annular structure than in the perpendicular direction (resp. solid line and bold asterisks Fig. 2, *right*). The superimposition of the two azimuthally averaged radial profiles shows that these profiles have a similar behaviour and are roughly a constant up to $\sim 2''$, then shows a strong discrepancy between $2''$ and $4''$. We assume then that the region up to $2''$ is free of significant resolved dust amount and that the scaling factor is $\sim 0.400 \pm 0.015$ (between $0.8''$ and $2''$).

3. Results

3.1. Orientation of the disk

Fig. 3 (*left*) shows the final reduced image of the disk and brings out the annular structure evidenced in the ratio of HD 141569 A to the reference star (Fig. 2). Unsubtracted secondary spider diffraction spikes are responsible for the bright areas inside the annulus. These patterns do not correspond to any realistic excess. An image of what would be observed without these spikes is shown in the bottom-right corner of the reduced image.

We computed the distance from the star corresponding to the maximum surface brightness of the annulus versus the position angle over a 90° range (Southern part of the disk). Least-squares ellipse fitting constrains the major axis of the observed annulus to be at a position angle of $355.4° \pm 1°$ and leads to an upper limit for the disk inclination from edge-on of $37.5° \pm 4.5°$ assuming that the disk is axisymmetrical with respect to the star. The fit is superimposed on the reduced image of the disk (Fig. 3, *right*) and agrees well with all the observed structure.

3.2. Surface brightness distribution and photometry

Both radial surface brightness profiles along the Northern and the Southern semi-major axis of the disk peak at 325 ± 10 AU from the star, according to the *Hipparcos* star distance of 99^{+9}_{-8} pc (Fig. 4). Discrepancies between the two profiles are due, inside $2.5''$ to the above-mentioned diffraction spikes, and outside $3.6''$ to an imperfect elimination of the blurred light from the stellar companions HD 141569 B and HD 141569 C.

We now focus on the Southern profile which shows more clearly the annular shape of the disk. Both inside and outside the peak at 325 AU, the surface brightness steeply decreases (FWHM $\sim$ 150 AU). The decline becomes smoother further than 420 AU. More precisely, Table 1 gives the steepness indexes which match the surface brightness for different ranges of distance from the star. The change of slope around $4.2''$ has to be confirmed. Indeed, this distance corresponds to the position of a different detector matrix, also we do not exclude that shading may have caused this effect (STScI 1997). Nevertheless, the disk is positively detected at least up to $6''$.

We performed the photometry of the disk on elliptic contours with semi-major axis between $2''$ and $9''$. We find a total scattered flux density of 4.5 ± 0.5 mJy (~ 13.5 mag), which must be considered as a lower value since the scattered light below the spider diffraction patterns is not taken into account.

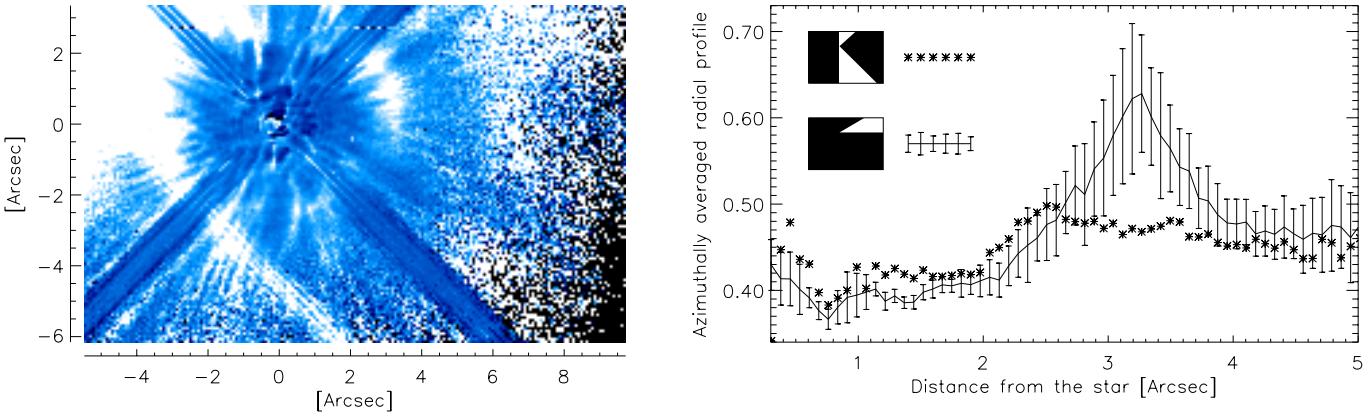

Fig. 2. *Left*: ratio of the HD 141569 A image to the reference star image assumed to be representative of the PSF. The image reveals an excess corresponding to the presence of circumstellar material well centered on the star. The top-left corner is blurred by the companions HD 141569 B and HD 141569 C. The mask has a radius of 0.3″ (∼ 4 pixels; the pixel size is about 0.076″). *Right*: two azimuthally averaged radial profiles. The small rectangular boxes mimic the left-hand image, with the white angular sectors illustrating the areas used to compute the profiles. Between $0.8''$ and $2''$, the signal to noise ratio in the profile plotted as asterisks is roughly a half the signal to noise ratio for the other profile.

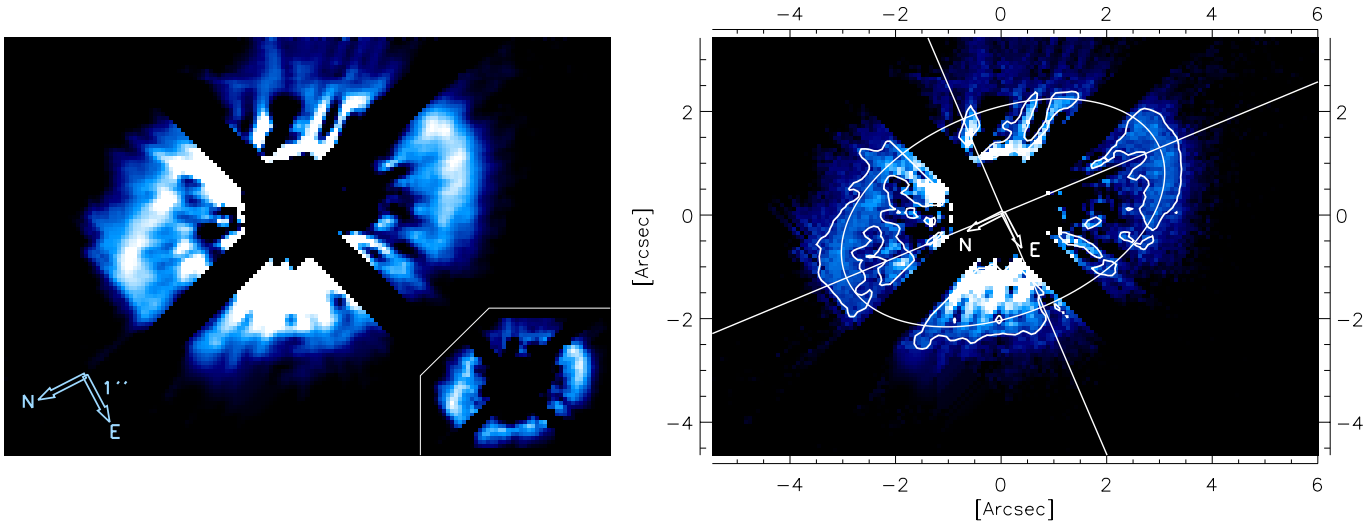

Fig. 3. *Left*: Scattered light image ($1.6\ \mu$m) of the HD 141569 A circumstellar disk in logarithmic scale. The scattered light due to the companions HD 141569 B and HD 141569 C and to their associated spider diffraction spikes (see Fig. 2) have been subtracted. In the bottom-right corner, we show the same disk where most of the unrealistic bright patterns close to the star (see text) have been removed so as to highlight the annular resolved structure. *Right*: Contours of the disk to allow comparison with the ellipse fitting superimposed on the image.

This corresponds to a ratio of scattered to stellar flux at 1.6 μm of about 2.2×10^{-3}.

4. Discussion

4.1. Disk properties

Assuming an optically thin ring and an inclination from edge-on of $35°$, we reproduce the main shape of the surface brightness along the major axis of the disk with an annulus peaked at 330 AU from the star and a radial surface dust distribution proportional to r^4 inside the peak and to $r^{-6.8}$ outside. This profile does not depend on the exact anisotropic scattering properties of the grains because it is measured along the major axis of the disk, *i.e.* where the scattering angle always close to $90°$. For simplicity, we have therefore assumed that grains scatter isotropically. The predicted surface brightness is superimposed in Fig. 4 on the observed one.

The dust population derived, assumed to be made of amorphous fluffy grains as described in Augereau et al. (1999a) larger than about a half micrometer, fits quite well the 20–100 μm SED but does not explain the shorter wavelength data. Emission features at 7.7 μm, 8.6 μm and 11.3 μm, tentatively attributed to aromatic molecules (e.g. Polycyclic Aromatic Hydrocarbons), have been detected by Sylvester et al. (1996a). The present model can not reproduce these features. Anyway, the presence of dust closer to the star is required to reproduce at least the 10 μm continuum. This second population is expected to be too close to the star (typically inside the first hundred AU) to be detectable in the present data. Such hot grains probably contribute to the 20 μm SED and may also be responsible for all

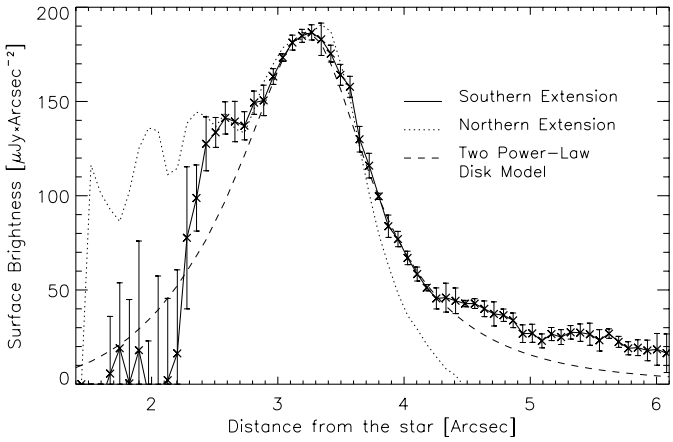

Fig. 4. Radial surface brightness distribution along the major axis of the disk. They have been obtained by azimuthally averaging the profiles over a 6 degree sector overlapping the major axis.

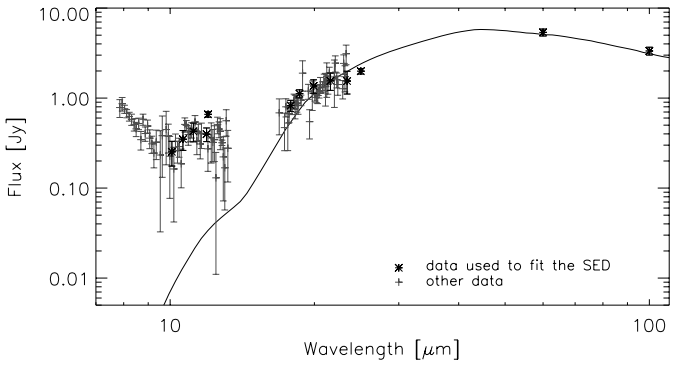

Fig. 5. Best fit of the 8–100 μm SED (IRAS and Sylvester et al. (1996a) measurements) taking into account the fact that the disk shapes an annulus. Grains are assumed to be made of silicate, organic refractories and H_2O ice and follow a collisional size distribution ($\propto a^{-3.5}$). The long wavelength continuum is well reproduced whereas the 10 μm predicted flux densities are about one order of magnitude smaller than the measured ones. This model suggests that an additional population of hot grains closer to the star is needed to account for the short wavelength excesses.

or part of the 12.5 μm and 17.9 μm extended emissions (0.75″ (75 AU) in radius) resolved by Silverstone et al. (1998). More data and modeling are needed to confirm that issue.

4.2. Comparison with HR 4796 A

It is particularly instructive to further compare HD 141569 A to HR 4796 A:

– both stars exhibit a circumstellar ring, but the HD 141569 A annulus is about 9–10 times wider than the HR 4796 A one,
– two dust populations are required to fit both full SEDs (Koerner et al. 1998; Augereau et al. 1999a),
– the inner edge of the HD 141569 A disk suggests a truncation process as already proposed for HR 4796 A,
– the outer disk distribution (further ∼325 AU) seems steeper than the spatial distribution of dust supplied by colliding or evaporating bodies (Lecavelier des Etangs et al. 1996) as for HR 4796 A. A perturbing body as a source for this outer truncation is possible. Nevertheless, no massive perturbing body is detected so far unlike for HR 4796 A.

Most of the above remarks regarding the properties and the dynamics of the HD 141569 A circumstellar disk will be further investigated in a forthcoming paper.

References

Augereau J.C., Lagrange A.M., Mouillet D., Papaloizou J.C.B., Grorod P.A., 1999, A&A, 348, 557
Corporon P., Lagrange A.M., 1999, A&AS 136, 429
Devillard N., "The eclipse software", The messenger No 87 - March 1997, web page: http://www.eso.org/eclipse/
Dunkin S.K., Barlow M.J., Ryan S.G., 1997, MNRAS 290, 165
Gahm G.F., Ahlin P., Lindroos K.P., 1983, A&AS 51, 143
Jayawardhana R., Fisher S., Hartmann L., Telesco C., Pina R., Fazio G., 1998, ApJ, 503, L79
Koerner D.W., Ressler M.E., Werner M.W., Backman D.E., 1998, ApJ, 503, L83
Lagrange A.M., Backman D., Artymowicz P., 1999, PPIV, in press
Lecavelier des Etangs A., Vidal-Madjar A. & Ferlet R., 1996, A&A 307, 542
Lindroos K.P., 1985, A&AS 60, 183
Malfait K., Bogaert E. and Waelkens C. 1998, A&A 331, 211
Pirzkal N., Spillar E.J., Dyck H.M., 1997, ApJ 481, 392
Schneider G., Smith B.A., Becklin E.E., Koerner D.W., Meier R., Hines D.C., Lowrance P.J., Terrile R.J., Thompson R.I., Rieke M, 1999, ApJL, 513, 127
Silverstone M.D., Weinberger A.J., Becklin E.E., Lowrance P.J., Zuckerman B., Marsh K.A., Koerner D.W., Werner M.W., Terrile R.J., Smith B.A., Schneider G., Rieke M.J., Thompson R.I., 1998, AAS, 193.7316S
STScI/NICMOS web page: "NICMOS Image Data ANOMALIES", http://www.stsci.edu/instruments/nicmos/nicmos_anomalies.html
Sylvester R.J., Skinner C.J., Barlow M.J., Mannings V., 1996, MNRAS 279, 915
Sylvester R.J., Skinner C.J., 1996, MNRAS 283, 457
van den Ancker M.E., de Winter D., Tjin A Djie H.R.E., 1998, A&A 330, 145
Weinberger A.J., Becklin E.E., Schneider G., Smith B.A., Lowrance P.J., Silverstone M.D., Zuckerman B., 1999, in preparation, to be submitted to ApJL
Yudin R.V., Evans A., 1998, A&AS 131, 401
Yudin R.V., Clarke D., Smith R.A., 1999, A&A 345, 547